World Journal of Innovation and Modern Technology E-ISSN 2756-5491 P-ISSN 2682-5910
Vol 9. No. 5 2025 www.iiardjournals.org online version

Biodiesel Synthesis and Characterization from Waste Castor Oil Seed Biomass Utilizing *Afzelia Africana* Seed Husk Derived Nano Catalyst for Enhanced Transesterification Efficiency

Udemba[1] Chinenye Margaret and Ezeh[2] Ernest Mbamalu
[1]Department of Chemical Engineering, Caritas University Amorji Nike Enugu, Nigeria
[2] Department of Chemical Engineering, Federal University, Otuoke, Bayelsa, Nigeria
Corresponding authors E-mail: ezehem@fuotuoke.edu.ng

DOI: 10.56201/wjimt.v9.no5.2025.pg166.197

Abstract

This study focused on the production of biodiesel from castor seed oil using Afzelia Africana seed husk ash (AASHA) as a heterogeneous catalyst. The physicochemical properties of the castor seed oil and the catalyst were characterized. The effects of process variables such as methanol/oil molar ratio, catalyst concentration, reaction temperature, reaction time, and agitation speed on the biodiesel yield were investigated. Response surface methodology (RSM) was employed to optimize the production process. The optimal conditions were found to be: methanol/oil molar ratio of 10.4:1, catalyst concentration of 2.19 wt%, reaction temperature of 63°C, reaction time of 1.5 hours, and agitation speed of 394 rpm, which resulted in a biodiesel yield of 90.9%. The properties of the produced biodiesel, such as density, viscosity, flash point, cetane number, and acid value, were within the American Society for Testing and Materials (ASTM) standards for biodiesel. Gas chromatography-mass spectrometer (GC-MS) analysis confirmed the conversion of the fatty acids in the castor seed oil to their corresponding methyl esters. The Fourier Transform Infrared Spectroscopy (FTIR) analysis further supported the successful transesterification of the oil. The study demonstrates the feasibility of using AASHA as an effective and eco-friendly catalyst for the production of high-quality biodiesel from castor seed oil.

***Keywords**: Castor seed oil; Afzelia Africana; Heterogeneous catalyst; Transesterification; Biodiesel*

1.0 Introduction

The increasing global demand for energy, coupled with the depletion of fossil fuel reserves and the adverse environmental impacts associated with their combustion, has necessitated the exploration of alternative energy sources. Among these alternatives, biodiesel has emerged as a promising renewable energy source due to its potential to reduce greenhouse gas emissions, enhance energy security, and promote sustainable agricultural practices (IRENA.,2018). Among the renewable fuels, the ones that are produced from inedible oilseeds or food waste as the sources are favoured by researchers because the use of such seeds or food waste will not affect the cost of edible oil. Such seeds will not be expensive, which results in reducing the overall energy cost (Jambulingam *et al*.,2019. Vegetable-based fuels are the main alternative sources for fossil-based fuels. Since these bioresources are used mostly in ordinary diesel engines, it is known as biodiesel (Malani *et al*.,2019). There is a variety of vegetable species from different climate regions, which have been used for this purpose including soybean, canola, sunflower, coconut, castor, palm, corn, cottonseed, etc. each of which can carry a special amount of oil with its specific characters. Another possible source is the waste of edible oil. In this case, the production seems to be more economic and efficient (Adebayo., 2011; Atadashi *et al*.,2010).

Biodiesel, a fatty acid methyl ester (FAME), can be produced from various feedstocks, including vegetable oils, animal fats, and waste oils. This research article focuses on the production and characterization of biodiesel from waste castor oil seed biomass, utilizing *Afzelia Africana*as a nano catalyst (Jayaraman et al.,2020). Biodiesel production typically involves the transesterification of triglycerides present in oils and fats, where they react with an alcohol (usually methanol or ethanol) in the presence of a catalyst to form biodiesel and glycerol (Atadashi *et al* 2012). The choice of feedstock significantly influences the production process, yield, and quality of the biodiesel. Various feedstocks can be utilized for biodiesel production, including commonly used oils: soybean, palm, and rapeseed oil. These oils are often preferred due to their high triglyceride content but can be expensive and may compete with food production. Animal Fats Tallow and lard are examples of animal fats that can be converted into biodiesel (Kim *et al*.,2018; Lathiyae *et al*.,2018). They are generally less expensive than vegetable oils but may have lower quality biodiesel characteristics. Used cooking oils and other waste oils are increasingly being recognized as viable feedstocks for biodiesel production. They offer several advantages, including lower costs, reduced environmental impact, and the potential to recycle waste materials.

The transesterification process can be catalyzed by either homogeneous or heterogeneous catalysts (Betiku *et al*.,2019; Sebastian *et al*.,2017). Homogeneous catalysts, such as sodium hydroxide or potassium hydroxide, are commonly used due to their effectiveness. However, they can lead to challenges such as soap formation and difficulty in separating the catalyst from the biodiesel. In contrast, heterogeneous catalysts, such as solid acids or bases, offer advantages in terms of ease of separation and reusability, making them an attractive option for biodiesel production (Bholoili *et al*.,2019; Lathiya *et al*.,2018)). The use of waste oils as feedstocks not only addresses the economic aspects of biodiesel production but also contributes to waste management and environmental sustainability. By converting waste oils into biodiesel, the reliance on virgin feedstocks is reduced, thereby minimizing the ecological footprint associated with biodiesel production (Delzeit.,2019; Ma *et al*.,2017)). Furthermore, the utilization of waste oils can help mitigate issues related to waste disposal and pollution.

Waste oils, particularly those derived from food processing and agricultural activities, have gained attention as viable feedstocks due to their abundance and low cost. Castor oil, derived from the seeds of the Ricinus communis plant, is particularly noteworthy due to its high oil content and unique fatty acid composition, which includes Ricinoleic acid, a monounsaturated fatty acid that imparts distinct properties to the resulting biodiesel (Esonye *et al*.,2019; Ezeh & Agu.,2024). Waste castor oil seed biomass refers to the residual material left after the extraction of oil from castor seeds (Changmai, *et al*. 2019). This biomass is often underutilized and poses disposal challenges. However, it is rich in nutrients and can serve as a valuable feedstock for biodiesel production. The utilization of waste castor oil seed biomass not only contributes to waste management but also enhances the sustainability of biodiesel production by reducing reliance on virgin feedstocks. Furthermore, the valorization of this biomass aligns with the principles of circular economy, promoting resource efficiency and minimizing environmental impact (Septiani *et al*.,2016).

In recent years, the development of nano catalysts has gained attention in the field of biodiesel production. Nano catalysts, due to their high surface area and unique properties, can enhance the efficiency of the transesterification process, leading to higher yields and lower reaction times (Chatterjee *et al*.,2017). The incorporation of nano catalysts, such as *Afzelia Africana*, seed husk into the biodiesel production process represents a novel approach that could significantly improve the overall sustainability and economic viability of biodiesel production from waste feedstocks.

The efficiency of the transesterification process is heavily influenced by the choice of catalyst. Traditional catalysts, such as sodium hydroxide and potassium hydroxide, have been widely used; however, they present several drawbacks, including the need for anhydrous conditions and the generation of wastewater (Cheng *et al*.,2016). In recent years, nano catalysts have gained prominence due to their high surface area, enhanced catalytic activity, and the ability to operate under milder conditions. *Afzelia Africana*, a plant species known for its unique properties, has been identified as a potential source of nano catalysts for biodiesel production (Taher *et al*.,2019; Talha *et al*.,2016)). The use of plant-derived nano catalysts not only reduces the environmental footprint of the production process but also enhances the overall sustainability of biodiesel production.

While there has been significant research on biodiesel production from various feedstocks, there is a lack of comprehensive studies focusing specifically on waste castor oil seed biomass. This feedstock is often overlooked despite its potential for biodiesel production. Most studies on biodiesel production utilize conventional catalysts, which may not be optimized for waste feedstocks (Dalvand *et al*.,2018). There is a need for research that explores the use of advanced catalysts, such as nano catalysts, to improve the efficiency and yield of biodiesel production. Although biodiesel quality is critical for its commercial viability, there is insufficient research on the physicochemical properties of biodiesel produced from waste castor oil seed biomass using innovative catalysts (De Oliveira *et al*.,1017). Understanding these properties is essential for assessing the suitability of biodiesel for various applications. The environmental benefits and economic feasibility of using waste castor oil seed biomass and nano catalysts in biodiesel production have not been thoroughly evaluated. Research is needed to assess the sustainability and cost-effectiveness of this approach compared to traditional methods (Da Silva César *et al*.,2019). The integration of nanotechnology in biodiesel production is still in its infancy. There is a gap in understanding how nano catalysts, such as *Afzelia Africana*, can be effectively utilized to enhance biodiesel production processes, particularly from waste feedstocks.

By addressing these gaps, the proposed research aims to contribute valuable insights into the production and characterization of biodiesel from waste castor oil seed biomass, ultimately promoting more sustainable and efficient biodiesel production methods. This research addresses the pressing need for sustainable energy solutions. By focusing on waste feedstocks, this study not only seeks to mitigate environmental challenges associated with waste disposal but also aims to enhance the efficiency and quality of biodiesel production through the application of advanced catalytic processes. The findings of this research are expected to contribute valuable insights into the development of economically viable and environmentally friendly biodiesel production methods, ultimately promoting the transition towards renewable energy sources and supporting global efforts to combat climate change.

2.0 Materials and Method

2.1 Materials

Castor seeds, reagents, glass wares, equipment including gas chromatography-mass spectrometer (GC-MS), Fourier transform infrared spectroscopy (FTIR), viscometer, magnetic hot plate, and soxhlet extractor. Design expert software version 12.0.

2.2 Method

2.2.1 Sample Preparation

Castor seeds (as shown in Figure 1) were procured from Ogbete main market in Enugu, Enugu State. Initial cleaning of the seeds involved the manual removal of dirt and foreign materials through handpicking. Following this, the seeds were de-shelled and subjected to oven-drying at 60°C for a duration of 7 hours to achieve a moisture-free state. After drying, the inner seed coat was separated from the seed kernels using a winnowing technique. Subsequently, the clean, dried seeds were ground using a mechanical grinder, following the methodology outlined by Ude & Onukwuli (2019a).

2.2.2 Extraction of Oil from Castor Seed Biomass

Oil extraction from the castor seeds was performed using a solvent extraction method. To evaluate the oil content, 5 kg of the dried, ground castor seeds were placed in a Soxhlet extractor with 3 liters of n-hexane. The mixture was vigorously shaken and then sealed to prevent evaporation of the n-hexane, allowing the contents to macerate for 24 hours. Following maceration, the dissolved oil was decanted from the slurry, which was subsequently filtered to obtain a clear filtrate. The filtrate was distilled at 65°C to recover the n-hexane and isolate the extracted oil.

The percentage oil content of the castor seeds was calculated using the following formula: Percentage Oil Yield = Weight of Oil Extracted/Weight of Seed Sample x 100 (1)

2.2.3 Characterization of Castor Oil Seed Biomass

The physicochemical properties of the extracted castor oil were characterized in accordance with the American Society for Testing and Materials (ASTM) 6751 (1973) methodology. Analytical equipment, including Gas Chromatography-Mass Spectrometry (GC-MS; QP2010 Plus, Shimadzu, Japan) and Fourier Transform Infrared Spectroscopy (FTIR; M530 Bulk Scientific), were employed to determine the fatty acid profile and identify the functional groups present in the oil, respectively.

2.2.4 Investigation of Process Parameters Affecting Biodiesel Yield

To evaluate the effects of various process parameters on the biodiesel yield from castor seed oil, a one-factor-at-a-time approach was utilized. In this methodology, one parameter was varied while all others were held constant. The five parameters examined included the molar ratio of methanol to oil, catalyst concentration, reaction time, reaction temperature, and agitation speed. This systematic variation allowed for a comprehensive understanding of how each factor influences the biodiesel yield.

Figure 1: Castor Seed

2.3 Synthesis of Nano catalysts from*Afzelia Africana*

The synthesis of nanocatalysts from *Afzelia Africana* involves a systematic approach encompassing extraction, synthesis, characterization, and evaluation of catalytic performance. The process begins with the collection of *Afzelia Africana* seed husks (as illustrated in Figure 2) from a pristine, uncontaminated environment to prevent contamination by extrinsic impurities. The collected plant material is then thoroughly rinsed with distilled water to eliminate any surface dirt or contaminants. Following this, the material is shade-dried at ambient temperature to preserve its structural integrity.

Once dried, the plant material is ground into a fine, homogeneous powder using a mortar and pestle. This powder is subsequently mixed with distilled water in a ratio of 1:10 (w/v) and stirred at room temperature for 24 hours with a magnetic stirrer to facilitate the extraction of biomolecules. The resulting mixture is then filtered through filter paper or a cellulose membrane to separate the solid residue from the liquid extract, which contains the desired biomolecules.

Next, metal salts (specifically silver nitrate for the production of silver nanocatalysts) are dissolved in distilled water to prepare the precursor solution. This metal salt solution is then combined with the liquid extract in a 1:1 ratio. The pH of the mixture was adjusted using mild acids or bases to optimize conditions for the subsequent reaction. The mixture is allowed to react under controlled temperature and stirring conditions, enabling the biomolecular reduction process that leads to the green synthesis of nanoparticles.

The progression of nanoparticle formation is monitored using UV-Vis spectroscopy, which facilitates the observation of characteristic plasmonic peaks indicative of nanoparticle formation. Following the reaction, the mixture is subjected to centrifugation to isolate the nanoparticles from the solution. The collected nanoparticles are washed with distilled water and ethanol to eliminate any unreacted materials and impurities. Finally, the purified nanoparticles are dried in an oven at a low temperature (60°C) to yield the nanocatalysts.

Figure 2: *Afzelia Africana* Seed Husk

2.4 Characterization of *Afzelia Africana* Nano catalysts

2.4.1 X-ray Diffraction (XRD)

X-ray Diffraction (XRD) serves as a pivotal technique for elucidating the crystalline structure, phase composition, and average crystallite size of synthesized nanocatalysts. The analysis begins with the preparation of the dried nanoparticles, which should be ground into a fine powder if they are not already in that form. This fine powder is then placed into a sample holder, where it is compacted uniformly. Proper compacting is crucial to minimize scattering effects that could interfere with the accuracy of the XRD measurements.

The XRD instrument is operated over a wide range of diffraction angles (2θ), typically from 5° to 90°. The use of Cu Kα radiation ($\lambda = 1.5406$ Å) is standard due to its optimal penetration depth and interaction with the sample's electron cloud, which results in effective diffraction patterns. The diffraction data is recorded, producing a pattern characterized by a series of peaks. These peaks correspond to the crystal planes of the synthesized nanoparticles, each representing distinct interplanar spacing defined by Bragg's law $n\lambda = 2d\sin\theta$. Here, n is an integer representing the order of the diffraction, λ is the wavelength of the X-ray, d is the distance between crystal planes, and θ is the Bragg angle.

Analysis of the recorded diffraction pattern involves indexing the peaks to identify the crystal phases present in the sample. This relationship enables the determination of lattice parameters, which are indicative of the crystal symmetry and unit cell dimensions. The full width at half maximum (FWHM) value reflects the extent of peak broadening, which is inversely related to crystallite size; sharper peaks indicate larger crystallite sizes, while broader peaks suggest smaller sizes. This detailed analysis facilitated by XRD not only confirms the successful synthesis of the nanocatalysts but also provides insights into their structural properties that are critical for understanding their catalytic performance.

2.4.2 Scanning Electron Microscopy (SEM)

Scanning Electron Microscopy (SEM) is an essential technique for examining the surface morphology, texture, and particle size distribution of synthesized nanocatalysts. The methodology for SEM analysis entails several critical steps to ensure accurate imaging and characterization.

The sample is prepared by placing a small quantity of dried nanoparticles on a conductive adhesive or aluminum stub, which provides a stable platform for imaging. If the nanoparticles are identified as non-conductive, it is imperative to enhance their conductivity by applying a thin layer of a conductive metal, such as gold or platinum, using a sputter-coating technique. This step mitigates the risk of charge accumulation during the imaging process, which can distort the electron emission and the resulting images. Once the sample is prepared, the stub is carefully loaded into the SEM chamber, where the chamber is then evacuated to establish a vacuum environment.

This vacuum is essential for minimizing air interference and improving the resolution of the imaging. During imaging, a focused beam of electrons is employed to systematically scan the surface of the nanoparticles. This focused electron beam interacts with the sample, causing secondary electrons to be emitted from the surface, which are then collected to form high-resolution images of the sample. The generated images are then analyzed to assess various surface features, including texture, roughness, and the degree of particle agglomeration. Additionally, the size distribution of the nanoparticles is measured by capturing images at multiple magnifications, with this multi-magnification approach facilitating a comprehensive understanding of particle size variability within the sample. By following this methodical approach, SEM effectively reveals crucial nanostructural information that is vital for correlating the physical characteristics of the nanocatalysts with their potential catalytic properties.

2.4.3 Fourier Transform Infrared Spectroscopy (FTIR)

Fourier Transform Infrared Spectroscopy (FTIR) is a vital analytical technique for identifying functional groups and confirming the presence of biomolecules that may be stabilizing the synthesized nanoparticles. The methodology for conducting FTIR analysis involves several systematic steps to ensure accurate sample preparation and data interpretation.

Prepare the sample by thoroughly mixing a precise amount of the dried nanoparticles with potassium bromide (KBr) to form a homogeneous mixture. This mixture should then be pressed into a pellet or formed into a thin film, depending on the specific requirements of the FTIR analysis. The preparation of a KBr pellet is crucial, as it provides a transparent medium for IR transmission while minimizing background interference.

Next, place the prepared pellet into the sample compartment of the FTIR spectrometer. The spectrometer should be calibrated prior to analysis to ensure the accuracy of the spectral data. Record the FTIR spectrum over a wide range of wavelengths, typically from 4000 cm^{-1} to 400 cm^{-1}. This range allows for the observation of various absorption bands corresponding to different vibrational modes of the molecular bonds present in the sample. Once the spectrum is obtained, analyze the resulting data by identifying the distinct peaks that appear in the spectrum. Correlate these observed peaks to their corresponding vibrational modes to determine the specific functional groups present within the sample. This analysis is crucial for confirming the presence of biomolecules that may be acting as stabilizers for the nanoparticles. The identification of these functional groups is significant, as it provides insights into the capping of nanoparticles by plant metabolites, which can influence their stability and catalytic properties. By employing this rigorous methodology, FTIR effectively elucidates the chemical characteristics of the synthesized nanocatalysts, aiding in the understanding of their potential applications.

2.4.4 Brunauer-Emmett-Teller (BET) Analysis

BET analysis measures the surface area and porosity of the synthesized nano catalysts, essential parameters for catalytic activity. Prepare the dried nanoparticles for analysis by degassing the sample to remove any adsorbed gases and moisture. Place the sample into the BET apparatus (often a gas adsorption instrument) Introduce nitrogen or another inert gas at liquid nitrogen temperature (approximately -196°C) to measure the amount of gas adsorbed on the surface of the nanoparticles. Analyze the data to calculate the specific surface area (m^2/g) using the BET equation, which relates gas adsorption to surface area.

Characterization of nano catalysts from *Afzelia Africana* provides critical insights into their structural, morphological, and functional properties. Each characterization technique contributes uniquely to understanding how these properties influence the catalytic performance of the nanoparticles. Employing a combination of techniques ensures that the synthesized nano catalysts are well-suited for their intended applications.

Synthesizing nano catalysts from *Afzelia Africana* leverage the natural biomolecules present in the plant for effective catalytic activity. By following this methodology, we produced, characterized, and evaluated sustainable nano catalysts thereby enhancing eco-friendly practices in nanomaterial synthesis.

2.5 Production of biodiesel by transesterification

Pre-treatment procedure was followed to reduce the excess free fatty acid of the oil below 1%. The oil samples were first heated on a heating mantle at 110˚C for 10 minutes for any available moisture to be driven off. The sample was cooled to 60°C in a water bath and then weighed into a 500ml three-necked round-bottomed flask. Then methanol of 60%w/w of oil mixed with concentrated sulphuric acid of 7% w/w of oil was added. A reflux condenser was fitted into the middle arm of the flask and water circulated at the outer jacket of the condenser (Eze et al.,2022; Ezekoye *et al*.,2019). A thermometer was inserted into the sample in the flask from one of the side arms. The whole setup was placed on a magnetic heating mantle and heated at 600C for 120 minutes at an agitation speed of 450rpm.

The mixture was then transferred into a 500ml separating funnel where it later separated into three layers comprising water at the bottom, pre-treated oil in the middle and methanol at the upper layer. The various components were carefully tapped off, water first, followed by the oil and finally methanol. Hot distilled water was poured into the oil in a separating flask, shaken and allowed to stand when it separated into water and oil layers below and above the flask respectively (Ani *et al*.,2024). The water was tapped off from the separating funnel and the pre-treated oil was poured into beakers and dried carefully in an oven regulated at a temperature of 105^0C until the residual water evaporated completely. After this process, the pre-treated oil was made ready for transesterification.

2.6 Catalyzed Production of biodiesel by transesterification

The oil was transesterified using methanol and nano catalysts from *Afzelia Africana*. A 500ml three-necked round-bottomed flask fitted with a condenser on the middle arm, a thermometer and a sample outlet on the side arms respectively served as the reactor. The heating system consists of an electromagnetic hot plate which heats the reactor and rotates the metal knob in the reactor through an electromagnetic field (Flach *et al*.,2015; Georgogianni *et al*.,2009). A specified quantity of the oil sample was introduced into the flask and the flask content was heated to the temperature established for the reaction. Then methanol and the catalyst mixture were added in the amount established for the reaction, and the stirrer switched on at a specified speed, taking this moment as zero time of the reaction. The reaction mixture was vigorously stirred and refluxed for the required reaction time (Gusniah *et al*.,2019). At the end of methanolysis, the transesterified product was made to stand for a day in a separating funnel where it separates into the upper biodiesel layer and the lower glycerol layer. The lower glycerol layer was tapped off first followed by the upper biodiesel layer.

2.7 Biodiesel purification by wet washing

After transesterification, the upper ester layer may contain traces of methanol and glycerol. The remaining unreacted methanol has a safety risk and might corrode engine components, and glycerin within the biodiesel will lessen the fuel lubricity and cause injector coking and other deposits. Such trace of methanol is soluble in water and is therefore removed by wet washing. The methyl ester or biodiesel layer was gently washed with hot distilled water in the ratio of 3:1 water to methyl ester. The methyl ester was gently washed to prevent its loss due to the formation of an emulsion that results in complete phase separation. The washed biodiesel was dried by heating at 105^{0}C on a laboratory hot plate until all residual water molecules evaporated.

The percentage biodiesel yield is given by the expression, % biodiesel yield = Volume of biodiesel produced÷ volume of oil used x 100 (2)

2.8 Determination of the fuel properties of castor oil seed biomass biodiesel.

The properties of the biodiesel fuel were characterized based on ASTM standards. The properties characterized include density, viscosity, cetane number acid value, calorific value and flash point. Iodine value, peroxide value, saponification value, free fatty acid value, molecular weight etc.

3.0 Result and Discussion

3.1 Physicochemical properties of castor oil seed biomass Oil

Table 1 presents the physicochemical properties of the raw oil extracted from castor seeds biomass. The oil exhibits a high acid number of 11.07 mg KOH/g and a free fatty acid (FFA) content of 5.53%. These values indicate the necessity for a pre-treatment step for the raw oil prior to the transesterification process using homogeneous catalysts; however, such pre-treatment may be bypassed when utilizing heterogeneous catalysts. The physicochemical properties of the castor seed oil are comparable to those of other non-edible oils, such as African pear seed oil (Onukwuli & Ude, 2018), Jatropha curcas oil), and Gmelina seed oil (Adebayo *et al*., 2011).

The oil's high density and viscosity present challenges for atomization in an internal combustion engine, indicating that it cannot be used directly as a biodiesel fuel. The iodine value of the oil, measured at 52.31 g/100 g, suggests a moderate level of unsaturation and characterizes it as a non-drying oil (Esonye *et al.*, 2019). A high saponification value also indicates that the oil is suitable for the production of household products such as liquid soap and shampoo, making it applicable for both domestic and industrial use. The peroxide value of the oil is assessed at 2.49 meq/kg, providing an indication of its rancidity. This relatively low peroxide value suggests that the oil has a good shelf-life and is capable of withstanding peroxidation during storage. The characterized physicochemical properties of castor oil seed biomass oil highlight its potential applications and the considerations necessary for its utilization as a biodiesel feedstock.

Table 1: Physicochemical Characteristics of Castor Oil Seed Biomass Oil

Properties	**Castor seed oil**
Density (g/cm^3)	0.9041
Kinematic viscosity at 40^{o}C (mm^2/s)	61.98
Saponification Value (mg/g)	165.68
Acid Value (mg/g)	11.07
Free Fatty Acid (%)	5.53
Iodine Value (g/100g)	52.31
Peroxide value (meq/kg)	2.49
Molecular weight (g/mol)	1088.51

3.2 Fatty acid profile of castor oil seed biomass Oil

The fatty acid composition/profile of castor seed oil was carried out with the aid of Gas Chromatography Mass Spectrometry (GC-MS). The fatty acid compositions of oil are shown in Table 2 and Figure 2 of Appendix A. From Figure 4.1 and Table 4.2, it can be observed that castor seed oil comprises 26.99% saturated acids (Lauric Acid, Myristics Acid, Palmitic acid and Stearic acid) and 73.01% unsaturated acids (Palmilitileic, oleic and linoleic). The dominant di-unsaturated fatty acid of the oil was oleic, which accounted for 60.12% of the total fatty acid content, hence, the oil belongs to the linoleic acid category. This shows that castor seed oil is highly unsaturated triglycerides (Triolein). Nevertheless, the fatty acid components of the castor seed oil were found to be consistent with the fatty acids present in typical oils used for producing biodiesel (Ude & Onukwuli.,.2019b).

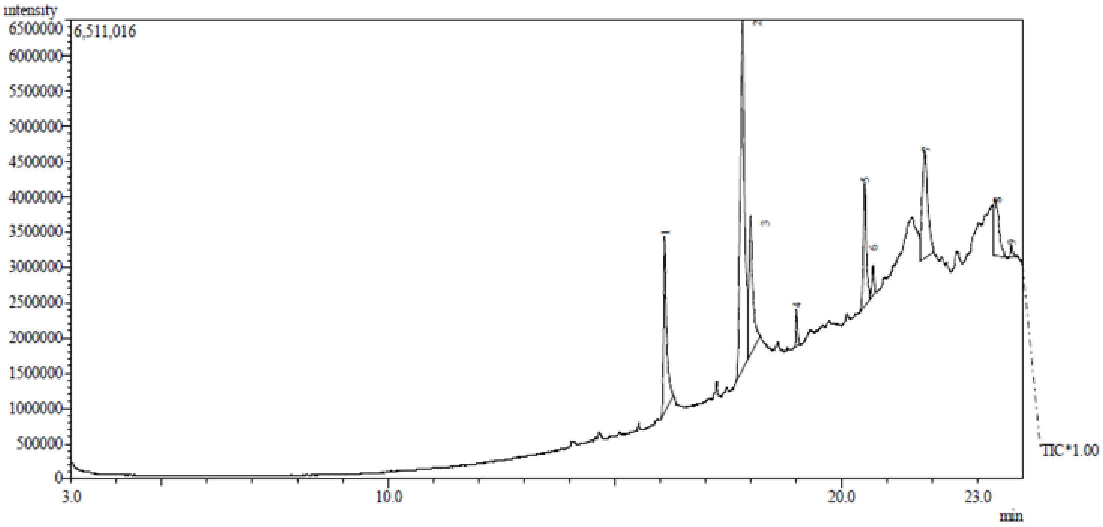

Figure 2: GC-MS of castor oil seed biomass Oil

Table 2: Fatty acid compositions of castor oil seed biomass oil.

S/N	**FFA Profile**		**Castor** oil **seed** biomass **oil**
	Fatty Acid	Component	Composition (%)
1	Lauric acid	C_{12}	0.89
2	Myristic acid	C_{14}	0.17
3	Palmitic acid	$C_{16:0}$	10.25
4	Palmitileic	C16:2	1.12
5	Stearic acid	$C_{18:0}$	15.68
6	Oleic acid	$C_{18:1}$	60.12
7	Linoleic acid	$C_{18:2}$	11.77
	Total		100

3.3 Fourier transform infra-red spectra of castor oil seed biomass oil

The FTIR spectrum of castor seed oil is shown in Figure 3. From the result, discernible peaks of note were recorded. The region 723.1 cm^{-1} – 913.2 cm^{-1} indicates the presence of =C-H(alkenes) functional groups. They possess bending types of vibrations appearing at low energy and frequency regions in the spectrum and they are all double-bounded. They are attributed to olefinic (alkenes) functional groups and are unsaturated. The characteristic peaks found in the region 1099.8cm^{-1} indicate stretching vibrations of C-O and C-O-C. They can also indicate the bending vibration of O-CH_3 in the spectrum (Onukwuli and Ude, 2018). The band region of 1237.8 cm^{-1} can be ascribed to the bending vibration of C-H methyl groups, while the band at 1379.1 cm^{-1} is ascribed to C=C bending vibrations. The region 1159-1461 cm^{-1} indicates the presence of an aromatic combination. Region 1744.2-2087.3 cm^{-1} indicates the presence of the O-H group stretched in carboxylic acid. The peaks at 2856.1 cm^{-1} and 2922.2 cm^{-1} indicate symmetric and asymmetric stretching vibrations of C-H alkane groups respectively. They could be methyl (CH_3) or methylene groups and they require high energy to cause stretching vibrations within their bond when compared to the ordinary C-H bending vibrations of alkene groups detected at low energy and frequency regions (Ude & Onukwuli, 2018). The peak at 3011.7 cm^{-1} with stretching mode of vibration is ascribed to the presence of O-H groups. They are single-bounded and at high-energy regions in the spectrum (Ude *et al*.,2020; Ume *et al*.,2024).

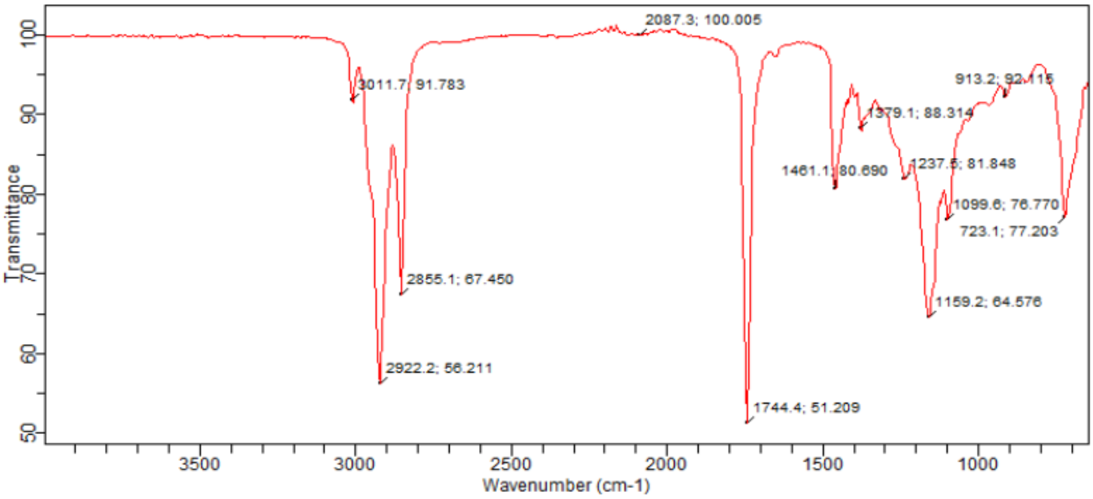

Figure 3: FTIR of castor oil seed biomass oil

3.4 Characterization of the Catalyst

3.4.1 BET analysis

The catalytic properties of the catalyst were determined with BET surface area analyser using BJH adsorption isotherm and presented in Table 3. From the table, it can be observed that the *Afzelia Africana* seed husk ash has good catalytic properties. The pore size is small and it has a high surface area.

Table 3: Catalytic properties of the *Afzelia Africana* seed husk ash catalyst

Parameters	***Afzelia Africana* seed husk ash**
Surface area (m^2/g)	404.117
Pore size (nm)	2.446
Total pore volume (cm^3/g)	0.198

3.4.2 Scanning electron microscopes (SEM) of the catalyst

The morphology of the catalyst was performed by SEM, as shown in Figure 4. The micrograph of the catalyst synthesized showed an increase in the number of pores and pore size on the clay. This supports the fact that it has more surface area with lower pore size.

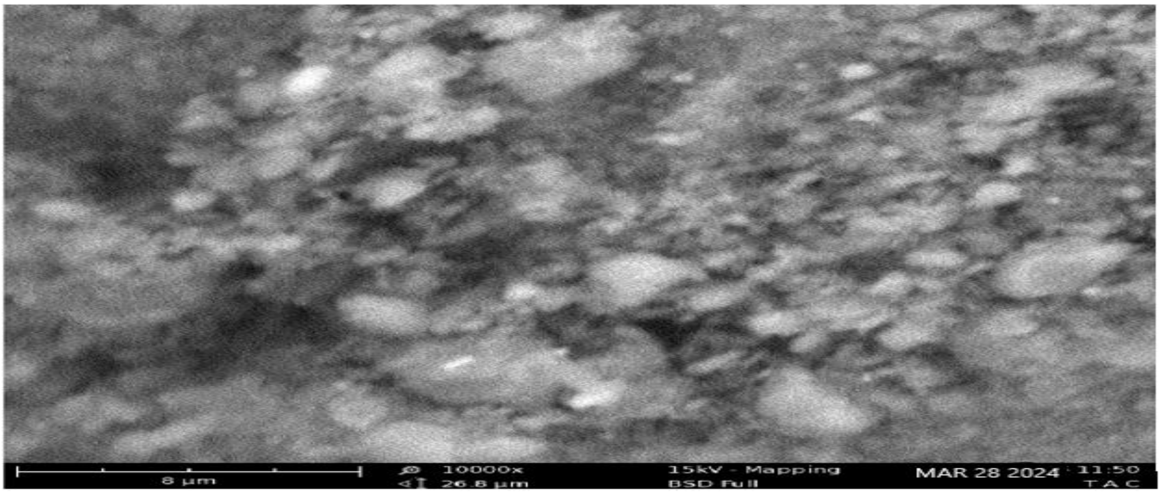

Figure 4: SEM image of the catalyst.

3.4.3 X-ray fluorescence analysis of the catalyst

The chemical composition of the catalyst used in this research is summarized in Table 4. The main compositions of the catalyst are Si, Al, Mg, Ca, K and Fe. It contains metallic oxides such as MgO, Al_2O_3, SiO_2, K_2O, CaO, TiO_2, Cr_2O_3, Mn_2O_3, Fe_2O_3, ZnO and SrO which are constituents of heterogeneous catalysts (Ude and Onukwuli, 2020). The high amounts of SiO_2, Al_2O_3 and Fe_2O_3 classify it as Brønsted and Lewis acids whose acidity and catalytic properties are largely dependent on the electronegativity of interlamellar spacing of exchangeable cations attached to the negatively charged aluminosilicate sheets (Moazeni *et al*., 2019).

Table 4: X-ray fluorescence (XRF) of catalyst

Elements	Catalyst
Na_2O	0.002
MgO	1.120
Al_2O_3	21.32
SiO_2	56.12
P_2O_5	0.302
SO_3	3.421
K_2O	0.321
CaO	0.121
TiO_2	0.079
Cr_2O_3	0.014
Mn_2O_3	0.024
Fe_2O_3	25.21
ZnO	0.022
SrO	0.032

3.4.4 X-ray diffraction pattern (XRD) of the catalyst

Figure 5a depicts the XRD of the catalyst and it shows that the *Azfelia Africana* seed husk ash contains graphite (carbon), quartz (SiO_2) and osumilite (K, Na, Fe, Mg, Al) confirming the presence of Alumina and silica and iron which are the characteristic element of catalyst. The crystalline nature of the catalyst was also observed to exist at 26° $2\theta°$ (Figure 5b).

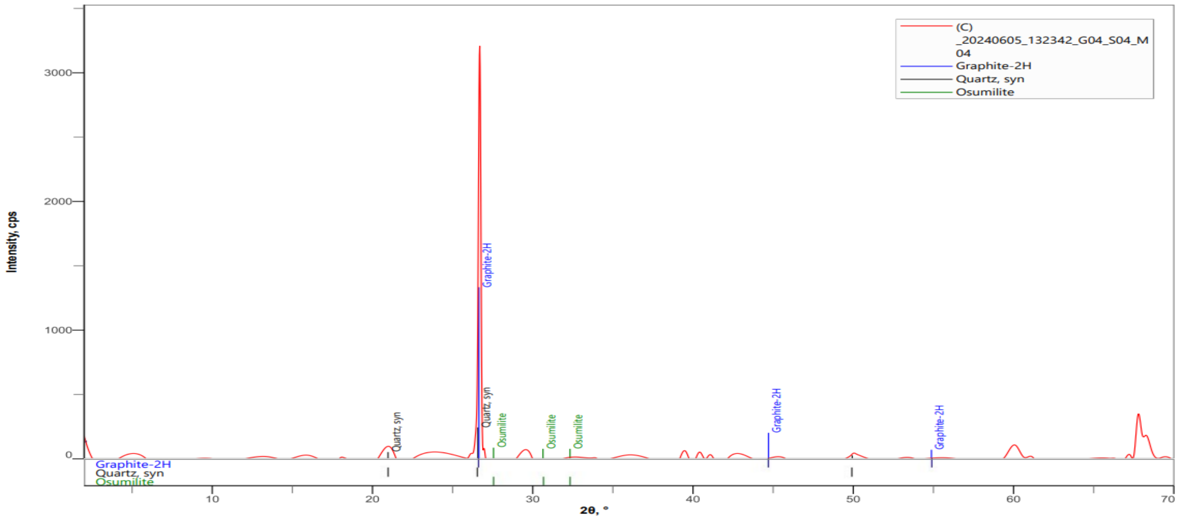

Figure 5a: XRD of catalyst.

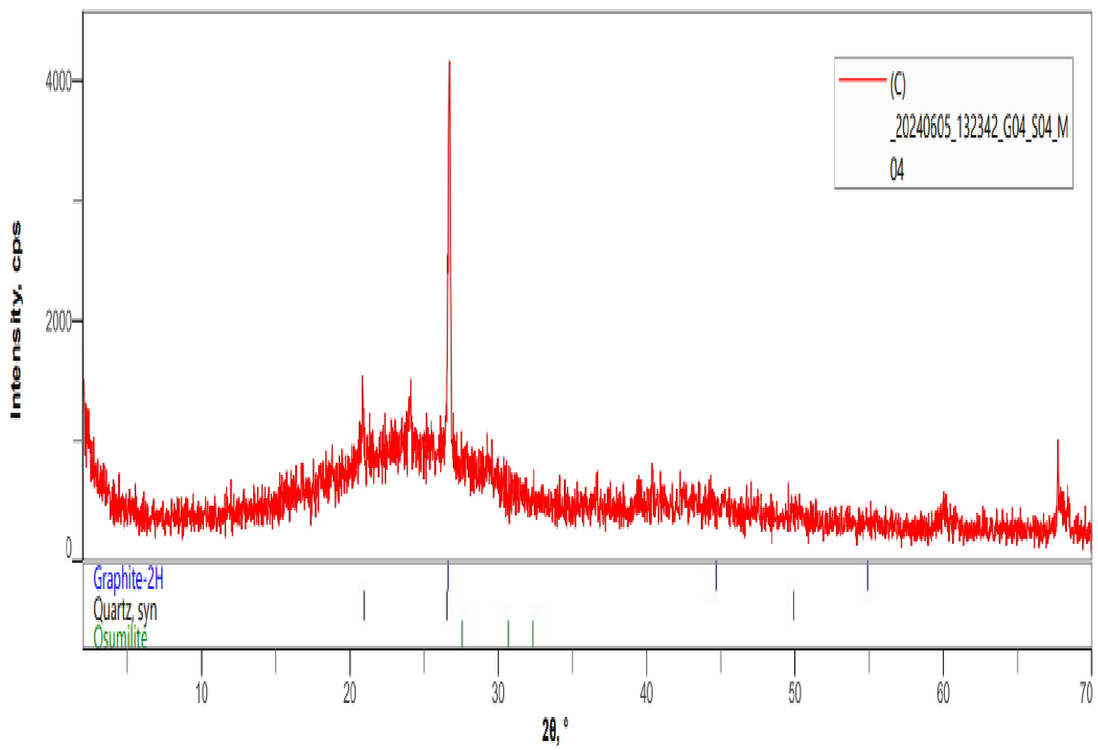

Figure 5b: Crystallinity position of catalyst.

3.5 Effects of Process Variables on the Biodiesel Yield

3.5.1 Effect of methanol/oil molar ration on yield

The alcohol-to-oil molar ratio is one of the most important factors that can affect the yield of esters. The stoichiometry of the transesterification reaction requires a 3:1 molar ratio to yield 3 moles of ester and 1 mole of glycerol, but most researchers have found that excess alcohol was required to drive the reaction close to completion. In this research, methanol was the preferred alcohol and the effect of its molar ratio in the range of 6:1 to 14:1 was investigated, keeping other process parameters fixed. The yield of methyl ester to the different molar ratios of methanol/oil catalysed by *Afzelia Africana* seed husk ash is shown in Figure 6a. The results indicated that the methanol oil molar ratio has a significant impact on biodiesel yield. The maximum ester yield was obtained at a methanol/oil molar ratio of 10:1 for both oils. The higher molar ratio resulted in a higher yield of ester. The yield reduced when the molar ratio was beyond 10:1. This could be that methanol has a polar hydroxyl group which acts as an emulsifier causing emulsification that made the separation of the ester layer from the water layer very difficult at high volume of the methanol thus, causing loss in the yield of the ester. The results obtained are in agreement with the reports of earlier works of Ude & Onukwuli 2018; Wancura *et al*.,2018).

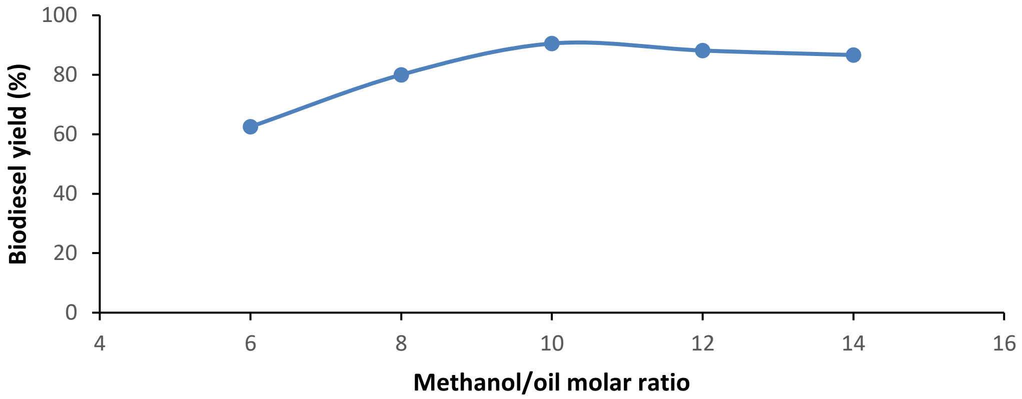

Figure 6a: Effect of Methanol/Oil Ratio on the Biodiesel Yield

3.5.2 Effect of catalyst concentration on biodiesel yield

The effect of catalyst concentrations expressed as a weight percentage of the castor seed oil on the production yield is presented in Figure 6b. From the figure, it could be observed that the yield of methyl ester increased with an increase in catalyst weight up to 2 wt% and then began to decrease. Initially, the amount of catalyst helped to accelerate the reaction by increasing the reaction rate. The higher yield of ester with an increase in catalyst weight is due to the higher availability of catalyst in the reaction medium. Increasing the catalyst weight beyond the catalyst weight of 2 wt% led to a decrease in ester yield. This may be due to excess catalysts causing dispersion and mixing problems, thereby inhibiting the formation of the end product (Moser., 2009).

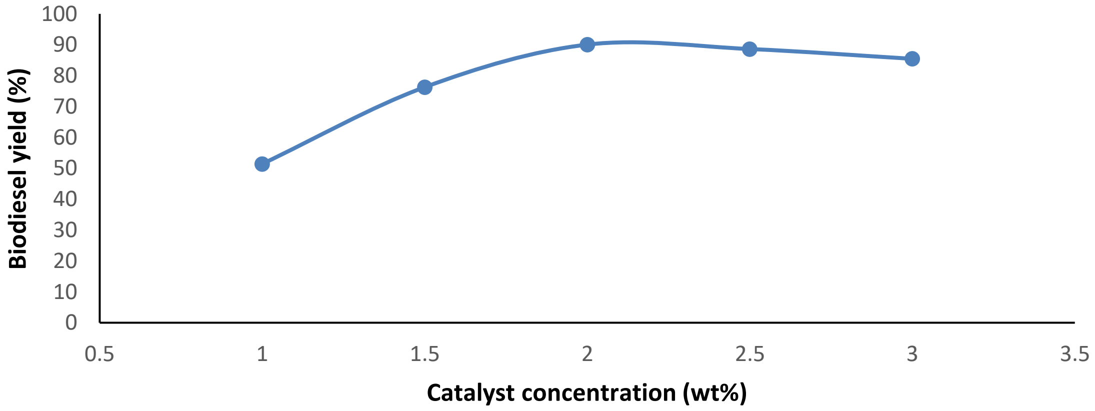

Figure 6b: Effect of Catalyst concentration (Catalyst wt%) on the Biodiesel Yield

3.5.3 Effect of temperature on biodiesel yield

Figure 6c depicts the effect of temperature on biodiesel yield of the transesterification reaction of castor seed oil with *Afzelia Africana* seed husk nanoparticle (AASH), the reaction temperature was varied as 50, 55, 60, 65 and 70^{o}C, while the other parameters were kept constant. As shown in Figure 6c, the reaction rate was slow at low temperatures, but biodiesel yield first increased and then decreased with the increase of the reaction temperature beyond 60^{o}C. Generally, a more rapid reaction rate could be obtained at high temperatures, but at high temperatures, methanol was vaporised and formed a large number of bubbles, which inhibited the reaction on the two-phase interface. A similar result was reported by Ude and Onukwuli, (2020).

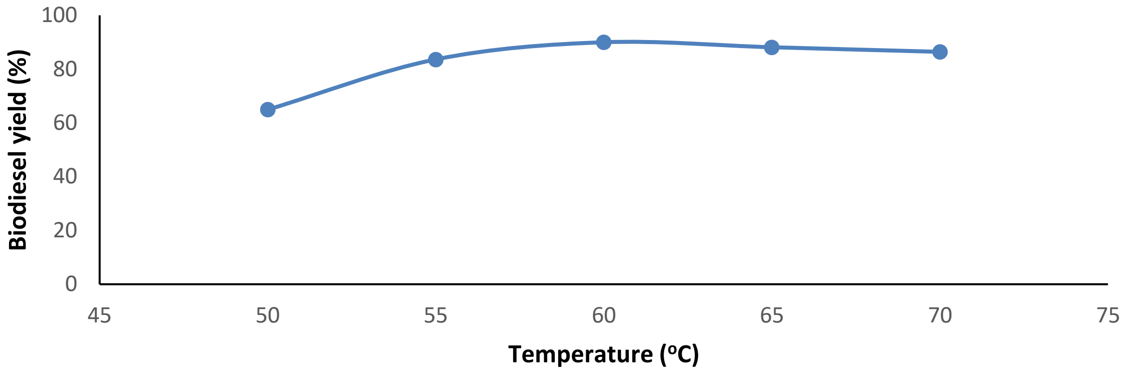

Figure 6c: Effect of Temperature on the Biodiesel Yield

3.5.4 Effect of time on biodiesel yield

The percentage yield of biodiesel increased with reaction time. In this work, the effect of reaction time from 0.5 to 2.5 hours on the reaction yield was investigated and shown in Figure 6d. It was found that higher yield occurred at a reaction time of 1.5 hours and beyond it the yields decreased (Figure 6d). The reaction was very slow due to the diffusion of methanol and triglyceride into the active site of the catalyst, and the decrease in the yield after 1.5 hours reported above may be due to a reversible reaction of transesterification resulting in the loss of esters.

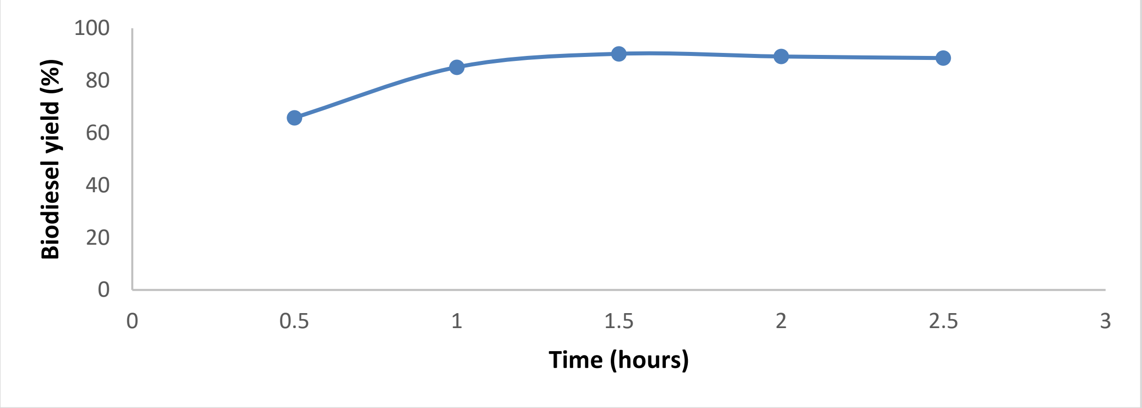

Figure 6d: Effect of Time on the Biodiesel Yield

3.5.5 Effect of agitation Speed on biodiesel yield

Mixing seems to be particularly crucial for the transesterification process because it provides homogeneity within the reaction mixture. It expanded the region in which oils came into touch with the catalyst or methanol solution (Orwa et al., 2009). The reaction is aided by mixing as well. In this investigation, stirring rates of 200, 300, 400, 500, and 600 rpm were used to conduct methanolysis (rpm). Figure 6e displayed the yield of methyl ester generated from castor seed oil using AASH catalyst at various rates of mixing. Figure 6e showed that the methanolysis reaction only produced a moderate yield at 200rpm and the yield rose as the stirring rate increased but decreased beyond 400rpm. This could be because homogeneity was attained when the mixing intensity was accelerated but at a higher speed beyond 400rpm the retention time for catalytic conversion was distorted.

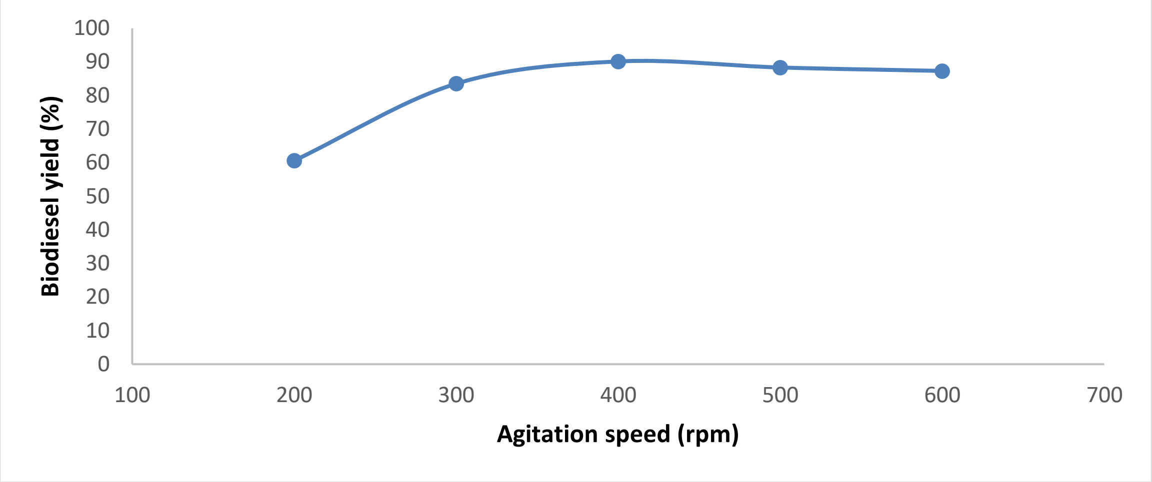

Figure 6e: Effect of agitation speed on biodiesel yield.

3.6 Statistical Analysis of Biodiesel Production from Castor Seed Oil Using Response

3.6.1 Surface Methodology

Central Composite Design (CCD) of Response Surface Methodology (RSM) in Design-Expert version 13 was employed to develop the model and statistically analyse the model for the production of biodiesel from castor seed oil using AASH.

3.6.2 Modelling of production

The experimental design employed was a two-level-four factor full factorial design, involving 32 experiments. Methanol/oil molar ratio, catalyst concentration, temperature, time and speed were selected as independent factors for the optimization study. The response chosen was the biodiesel yield. The response surface design table for the transesterification study is given in Table 5 and the responses are presented in Table 6. The model developed by the software in terms of coded values is shown in Equation 3, for the yields from Castor oil seed biomass.

$$Y_{Castor\ seed\ oil\ biodiesel\ yield\ (CSOB)} = 89.29 - 0.4042A + 3.73B + 4.10C + 1.69D + 0.1950E + 0.4438AB + 0.7675AC + 0.2813AD - 0.3438AE + 0.1438BC - 0.4675BD - 0.5425BE - 2.54CD - 0.5188CE - 0.3075DE - 0.5985A^2 - 5.02B^2 - 3.92C^2 - 2.66D^2 - 2.91E^2 \qquad (3)$$

where $\mathrm{A} = \frac{\mathrm{methanol}}{\mathrm{oil}}\,\mathrm{molar\ ratio}\ \left(\frac{\mathrm{mol}}{\mathrm{mol}}\right)$,
$\mathrm{B} = \mathrm{Catalyst\ concentration\ (wt\%)}$,
$\mathrm{C} = \mathrm{Temperature\ (°C)}$,
$\mathrm{D} = \mathrm{Time\ (Hour)}$,
$\mathrm{E} = \mathrm{agitation\ speed\ (rpm)}$, they are all in coded form

3.6.3 Adequacy analysis of the model

The analysis of variance for the model of the transesterification process parameters is shown in Table 5. From the table, it could be observed that all the five variables: methanol/oil molar ratio (A), catalyst conc. (B), reaction temperature (C), time (D) and speed (E) have a significant effect on yield. The above model represents the quantitative effect of the factors (A, B, C, D and E) upon the responses (Y). Coefficients with one factor represent the effect of that particular factor while the coefficients with more than one factor represent the interaction between those factors. The positive sign in front of the terms indicates a synergistic effect while the negative sign indicates an antagonistic effect of the factor. The adequacy of the above-proposed models was tested using the Design Expert model test statistics. From the statistics test, the coefficients of determination ($R^2 = 0.9989$) are high, and the adjusted R^2 (0.9968) are in close agreement with the predicted R^2 (0.9969) values. The standard deviation of 0.4836 indicates that the data points are closer to the mean value of 77.95. The lower coefficient of variation (C.V) of 0.6204 % shows higher precision. The high adequate precision of 78.1664 indicates that model prediction is reliable. The test is shown in Table 7.

Table 5: ANOVA for Castor Seed Oil Biodiesel (CSOB) Yield

Source	**Sum of Squares**	**df**	**Mean Square**	**F-value**	**p-value**	
Model	2296.23	20	114.81	490.92	< 0.0001	significant
A-Methanol/oil molar ratio	3.92	1	3.92	16.76	0.0018	
B-Catalyst conc.	333.91	1	333.91	1427.76	< 0.0001	
C-Temperature	402.62	1	402.62	1721.55	< 0.0001	
D-Time	68.95	1	68.95	294.83	< 0.0001	
E-Agitation speed	0.9126	1	0.9126	3.90	0.0738	
AB	3.15	1	3.15	13.47	0.0037	
AC	9.42	1	9.42	40.30	< 0.0001	
AD	1.27	1	1.27	5.41	0.0401	
AE	1.89	1	1.89	8.08	0.0160	
BC	0.3306	1	0.3306	1.41	0.2595	
BD	3.50	1	3.50	14.95	0.0026	
BE	4.71	1	4.71	20.13	0.0009	
CD	103.53	1	103.53	442.68	< 0.0001	
CE	4.31	1	4.31	18.41	0.0013	
DE	1.51	1	1.51	6.47	0.0273	
A^2	10.51	1	10.51	44.93	< 0.0001	
B^2	740.25	1	740.25	3165.21	< 0.0001	
C^2	451.56	1	451.56	1930.81	< 0.0001	
D^2	207.71	1	207.71	888.14	< 0.0001	
E^2	248.57	1	248.57	1062.86	< 0.0001	
Residual	2.57	11	0.2339			
Lack of Fit	0.1638	6	0.0273	0.0567	0.9984	not significant
Pure Error	2.41	5	0.4818			
Cor Total	2298.80	31				

Std. Dev.	0.4836	R^2	0.9989
Mean	77.95	Adjusted R^2	0.9968
C.V. %	0.6204	Predicted R^2	0.9969
		Adeq Precision	78.1664

Table 6: RSM results of the effects of process variables on the biodiesel yield from castor seed oil

Std	**A: Methanol/oil molar ratio**	**B: Catalyst conc.**	**C: Temperature**	**D: Time**	**E: Agitation speed**	**Yield**
		wt %	Deg. Cel.	Hours	rpm	%
1	8	1.5	55	1	500	65.64
2	12	1.5	55	1	300	58.72
3	8	2.5	55	1	300	70.13
4	12	2.5	55	1	500	69.07
5	8	1.5	65	1	300	74.32
6	12	1.5	65	1	500	74.65
7	8	2.5	65	1	500	82.77
8	12	2.5	65	1	300	84.94
9	8	1.5	55	2	300	71.29
10	12	1.5	55	2	500	70.52
11	8	2.5	55	2	500	78.14
12	12	2.5	55	2	300	77.52
13	8	1.5	65	2	500	74.12
14	12	1.5	65	2	300	74.7
15	8	2.5	65	2	300	80.62
16	12	2.5	65	2	500	80.45
17	6	2	60	1.5	400	87.6
18	14	2	60	1.5	400	85.98
19	10	1	60	1.5	400	61.63
20	10	3	60	1.5	400	76.55
21	10	2	50	1.5	400	65.3
22	10	2	70	1.5	400	81.68
23	10	2	60	0.5	400	75.15
24	10	2	60	2.5	400	81.93
25	10	2	60	1.5	200	77.15
26	10	2	60	1.5	600	77.93
27	10	2	60	1.5	400	88.55
28	10	2	60	1.5	400	88.6
29	10	2	60	1.5	400	89.1
30	10	2	60	1.5	400	89.5
31	10	2	60	1.5	400	90.1
32	10	2	60	1.5	400	90.1

The ANOVA result for the model terms given in Table 5 was applied to estimate the significance of the models at a 5% significance level. A model is considered significant if the p-value (significance probability value) is less than 0.05. From the p-values presented in Table 5, it can be stated that all the linear terms A, B, C, and D; the interactive terms AB, AC, AD, AE, BD, BE, CD, CE and DE for CSOB yield and interactive terms AB, AC, BD and all the quadratic terms A^2, B^2, C^2, D^2 andE^2 are significant model terms. Based on these assertions, the model equations were reduced to Equation 4.

$$Y_{Castor\ seed\ oil\ biodiesel\ yield\ (CSOB)} = 89.29 - 0.4042A + 3.73B + 4.10C + 1.69D + 0.1950E + 0.4438AB + 0.7675AC + 0.2813AD - 0.3438AE - 0.4675BD - 0.5425BE -$$

$$2.54CD - 0.5188CE - 0.3075DE - 0.5985A^2 - 5.02B^2 - 3.92C^2 - 2.66D^2 - 2.91E^2$$
(4)

The predicted R^2 value agreed reasonably with the adjusted R^2 value. The fitness of the model equation was validated using the coefficient of regression, R^2. The high R^2 value implied that the variability in the response can be explained by the model. The Predicted vs Actual plots presented in Figure 7 were used to check the distribution of residuals. The close distribution of the points along the straight lines indicates a good relationship between the experimental value and the predicted value of the response. This plot also confirms that the chosen model was adequate for the prediction of the response variable in the experimental value.

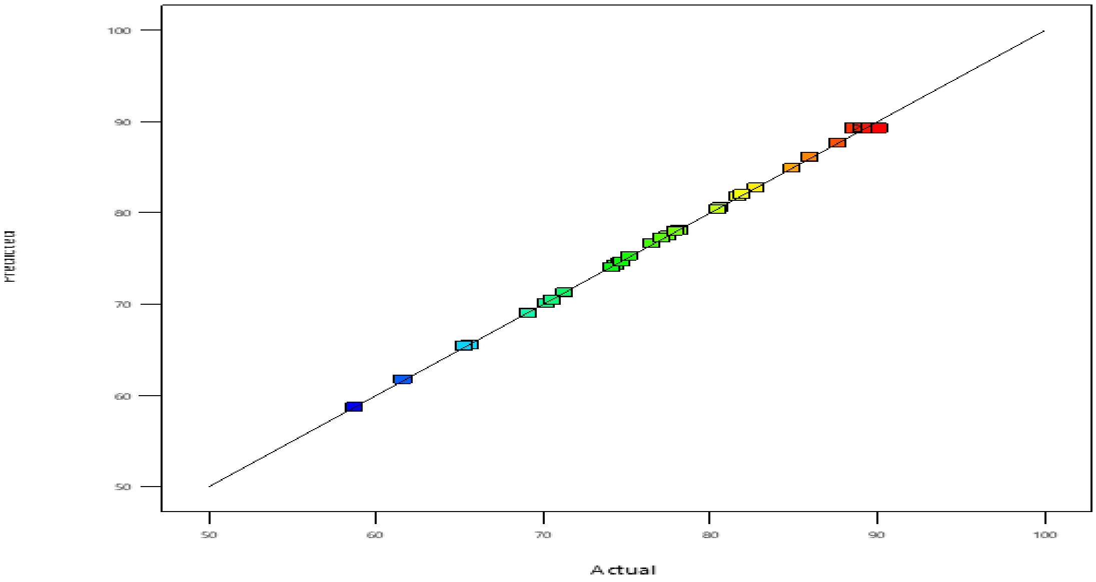

Figure 7: Predicted vs actual values of biodiesel yield.

3.6.4 Response surface plots of the models

Figures 8a to 8i are the surface plots of the predicted biodiesel yield which can be generated by Equations 3 and 4. The interaction effects of methanol/oil molar ratio and catalyst concentration on yields of biodiesel are shown in Figure 8a. It could be observed from the figures that the effect follows a similar trend on the yield. The Figures show that the amount of methyl ester yield increased with methanol/oil molar ratio and catalyst concentration. However, at higher catalyst concentrations and methanol/oil molar ratio, a reduction in the yield can be observed which may be due to mass transfer limitations and increased instability of the oil phase resulting in phase separation and emulsification.

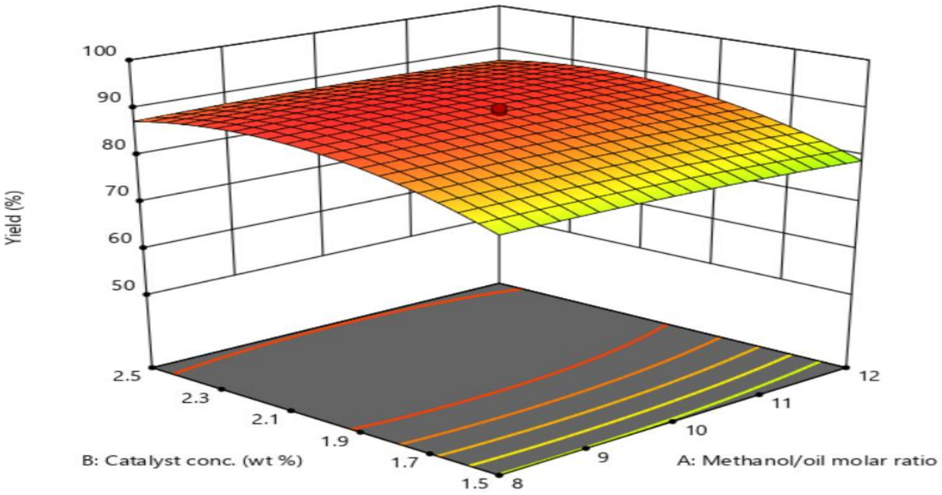

Figure 8a: Interactive effect of methanol/oil molar ratio and catalyst concentration on yield.

The interaction effects of the methanol/oil molar ratio and reaction temperature on the yield of biodiesel are shown in Figure 8b. At lower temperatures, below 60°C, the yield increases with methanol/oil molar ratio. However, at a temperature above 60°C, there was a reduction in yield. This may be a result of the evaporation of methanol which inhibits the reaction on the three-phase interface.

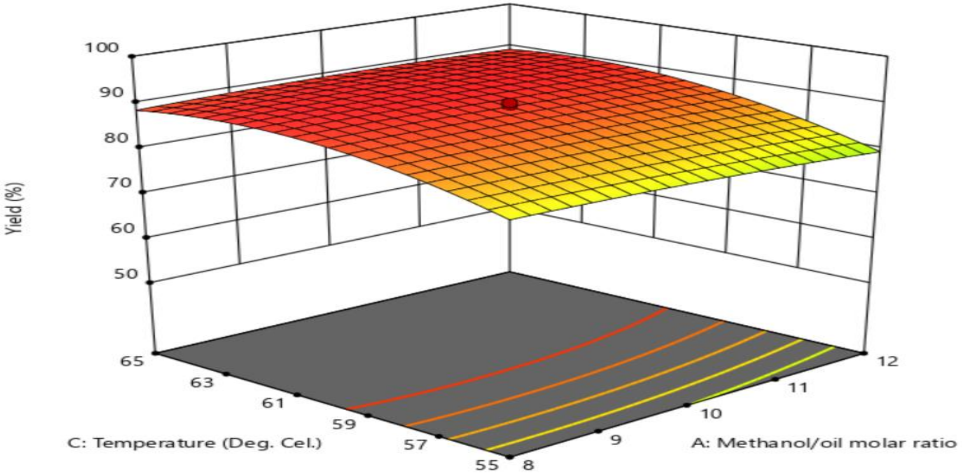

Figure 8b: Interactive effect of methanol/oil molar ratio and temperature on yield

The interaction effect of the methanol/oil molar ratio and time on the yield of biodiesel is shown in Figure 8c. The figure indicates that the amount of biodiesel yield increases with the methanol/oil molar ratio and reaction time. This may be a result of adequate time provided for conversion of the triglyceride. At a higher methanol/oil molar ratio and reaction time, a reduction in biodiesel yield can be observed due to reversible reaction at excess alcohol.

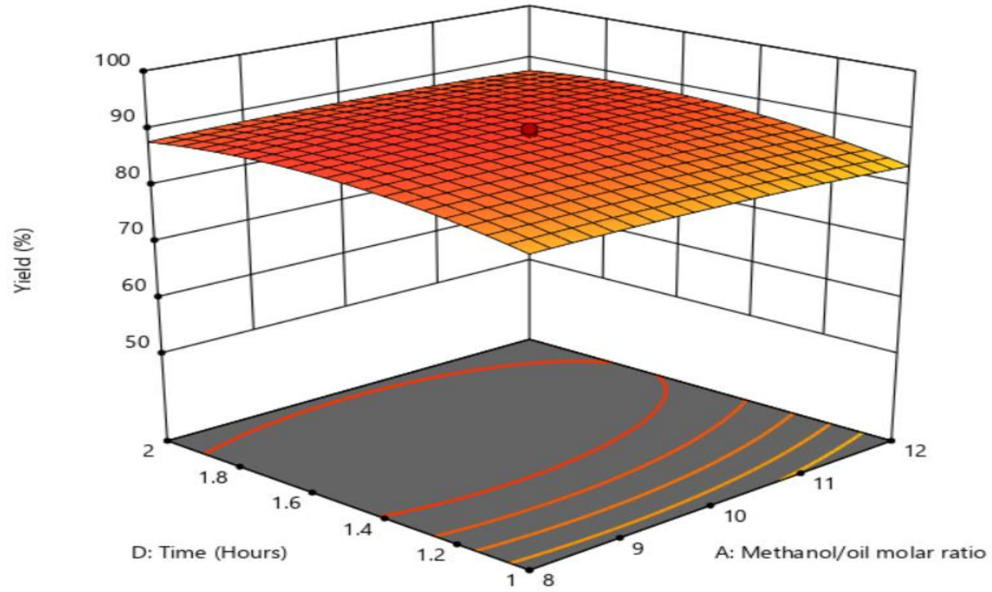

Figure 8c: Interactive effect of methanol/oil molar ratio and time on yield

The synergistic effect of methanol/oil molar ratio and agitation speed on the yield of biodiesel is shown in Figure 8d. The figure shows that the biodiesel yield increases with methanol/oil molar ratio and agitation speed as a result of a positive significant effect of methanol/oil molar ratio-agitation speed interaction term, AD on response. However, at a higher methanol/oil molar ratio and agitation speed, a reduction in the yield can be observed since the high speed could not allow further conversion of triglyceride.

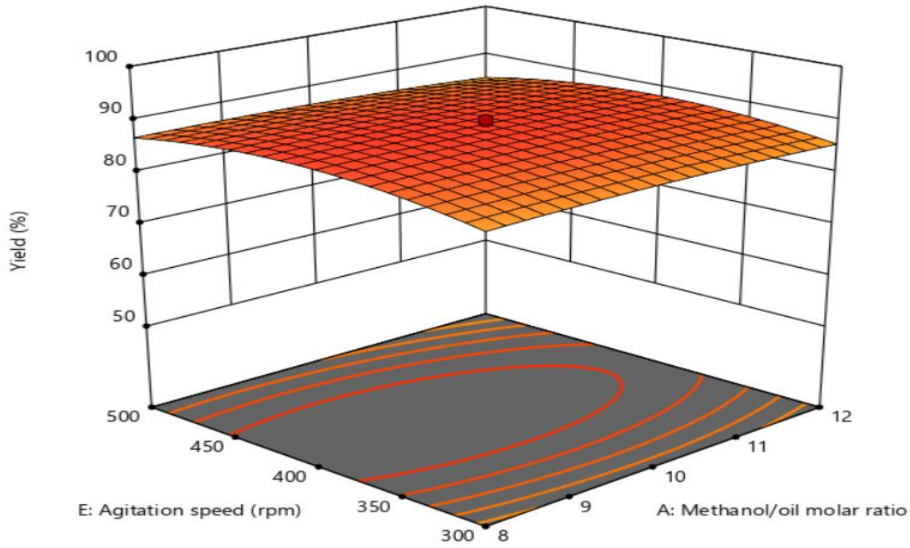

Figure 8d: Interactive effect of methanol/oil molar ratio and agitation speed on yield

The interaction effect of catalyst concentration and time on the yield of biodiesel is shown in Figure 8e. The figure indicates that the yield increases as reaction time and catalyst concentration increases but decreases at higher time and catalyst concentrations above 1.5 hours and 2 wt%. This could be due to catalyst deactivation, mass transfer limitation and instability of the oil phase.

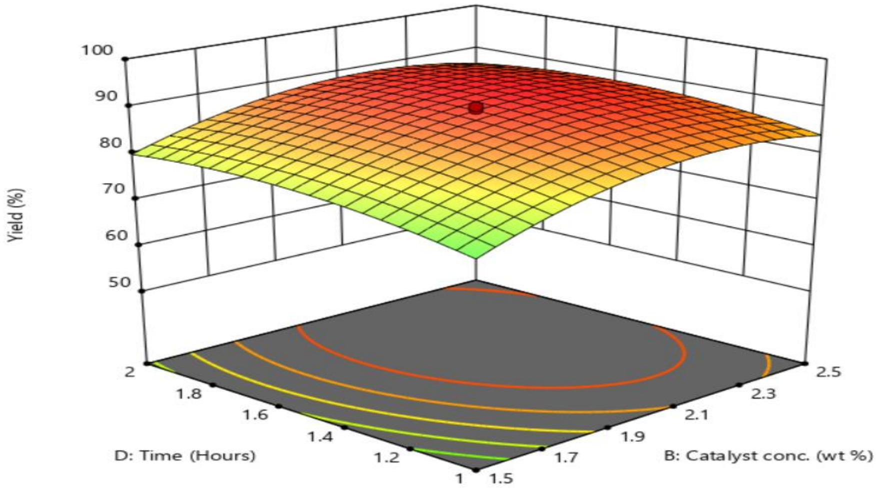

Figure 8e: Interactive effect of catalyst concentration and time on yield.

The interaction effect of catalyst concentration and agitation speed on the yield of biodiesel is shown in Figure 8f. The figure shows that the biodiesel yield increases with catalyst conc. And agitation speed as a result of a positive significant effect of catalyst dosage-agitation speed interaction term, BE on the response. However, at higher catalyst dosage and agitation speed, a reduction in the yield can be observed since the quadratic terms of the two factors are more significant with a negative effect and the high speed could not allow further conversion of triglyceride.

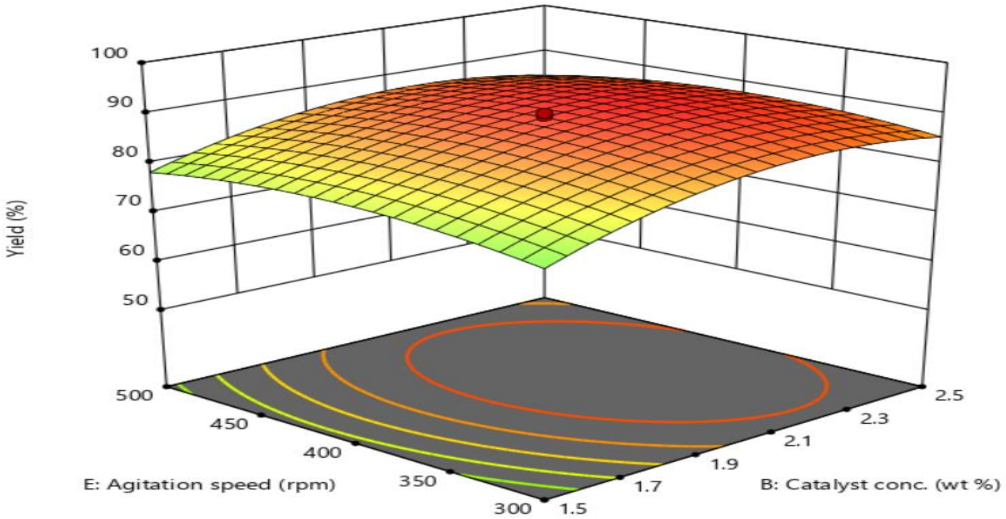

Figure 8f: Interactive effect of catalyst concentration and speed on yield.

The interaction effect of reaction temperature and time on the yield of biodiesel is shown in Figure 8g. At lower temperatures, below 60°C the yield increased with an increase in time. However, at a temperature above 60°C, there was a reduction in yield. This may be a result of the evaporation of methanol which inhibits the reaction on the three-phase interface.

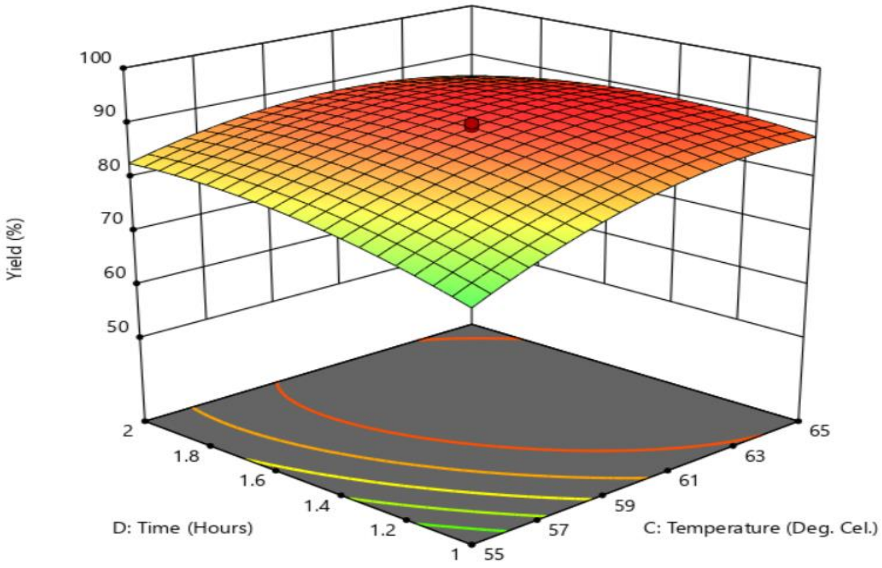

Figure 8g: Interactive effect of temperature and time on yield.

The interaction effect of reaction temperature and agitation speed on yield is shown in Figure 8h. The figure indicates that the yield of biodiesel increases with reaction temperature and agitation speed. However, at higher reaction temperature and agitation speed, there was a decrease in FAME yield because there is a negative significant effect of reaction temperature-agitation speed interaction term, (CE) on the response.

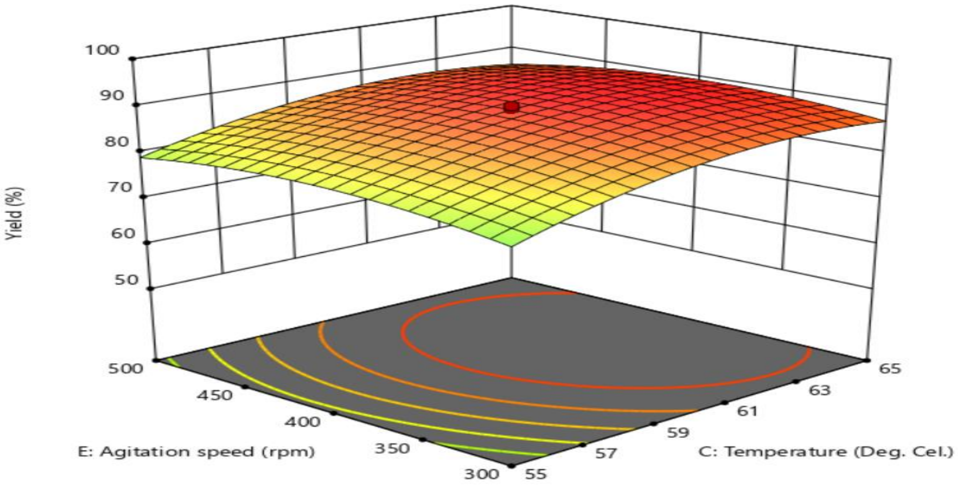

Figure 8h: Interactive effect of temperature and speed on yield.

The interaction effects of time and agitation speed on the yield of biodiesel are shown in Figure 8i. The figure indicates that the yield of biodiesel increases with an increase in reaction time and agitation speed. However, at higher reaction time and agitation speed, there was a reduction in biodiesel yield which may be attributed to the reversible reaction of transesterification resulting in loss of esters and re-introduction of unsaturated fatty acid.

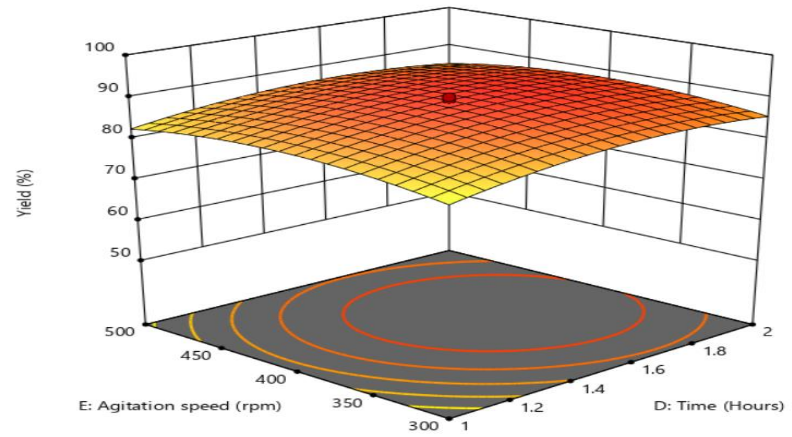

Figure 8i: Interactive effect of time and speed on yield.

3.7 Optimization of CSOB Biodiesel Production Process Parameters

A transesterification reaction under the obtained optimum operating conditions was carried out to evaluate the precision of the quadratic model; the experimental value and predicted values are shown in Table 7. Comparing the experimental and predicted results, it can be seen that the error between the experimental and predicted is less than 1% with a desirability of 0.997, therefore it can be concluded that the generated model has sufficient accuracy to predict the amount of biodiesel yield.

Table 7: Results of the model validation (experiment 1 indicates the optimum reaction conditions and yield)

Experiment	**CSOB**
Methanol/oil molar ratio A	10.4:1
Catalyst conc.(%wt oil) B	2.19
Temperature (^{o}C) C	63
Time (Hour) D	1.5
Speed (rpm) E	394
Experimental Yield (%)	90.9
Predicted yield (%)	91.11
Error (%)	0.23
Desirability	0.997

3.8 Characterization of CSOB Biodiesel Produced at Optimal Conditions

3.8.1 Fuel Properties

Table 8 presents a summary of all the biodiesel properties analysed and the limits that they were compared with (ASTM D 6751 (2002) standards). The density of the CSOB evaluated at 30 ^{o}C was within the ASTM limits for biodiesel. The viscosity of the oil was observed to reduce after the transesterification reaction and within the ASTM limits (1.6-6.0Cst) for biodiesel. The typical flash point of pure methyl ester is >200°C, classifying them as “non-flammable”. However, during the production and purification of biodiesel, not all the methanol may be removed, making the fuel flammable and dangerous to handle and store if the flash point falls below 130°C. The flash point of the CSOB was greater than 130°C, which falls within the ASTM standard and makes them safe for storage.

High fuel acidity is linked with corrosion and engine deposits. The CSOB has an acid value <0.5mgKOH/g. The ASTM value for TAN is 0.8 mgKOH/g; this implies that the acid values of the biodiesel are acceptable. The cetane number serves as a measure of ignition quality. Fuels with low cetane numbers show an increase in emission due to incomplete combustion. The lower limit for cetane index is 47 by ASTM standards. The cetane number of the CSOB was >47, which is above the lower limit for cetane number. Hence, the results obtained are acceptable.

Table 8: CSOB Biodiesel properties compared with ASTM limits

PROPERTY	UNITS	ASTM METHODS	CSOB Biodiesel	ASTM LIMITS
Density	kg/m^3	ASTM D-1298	876	830-880
Kinematics Viscosity	Cst	ASTM D-445	3.65	1.6-6.0
Flash Point	°C	ASTM D-93	180	≥130
Pour Point	°C	ASTM D-97	-10	+15 max
Cloud Point	°C	ASTMD-2500	-6	-15 to 5
Acid Value	mgKOH/g	ASTMD-974	0.43	≤ 0.80
Low Heating Value	MJ/kg		40	≥ 35
Aniline Point	(°C)	ASTM D-4737	188	
Cetane number		ASTMD-130	50	47

3.8.2 GC-MS Analysis of the CSOB Biodiesel

The CSOB produced using the optimal conditions was analyzed using GC-MS to confirm the conversion of fatty acids of the oil to methyl ester. The chromatogram of CSOB is depicted in Figure 9 and presented in Table 9. From the figure, it is observed that the major fatty acids were present in the oil at a retention time of 18 minutes while Table 9 shows that the fatty acids of their respective oils were converted to methyl esters. This implied that oleic acid was converted to oleate.

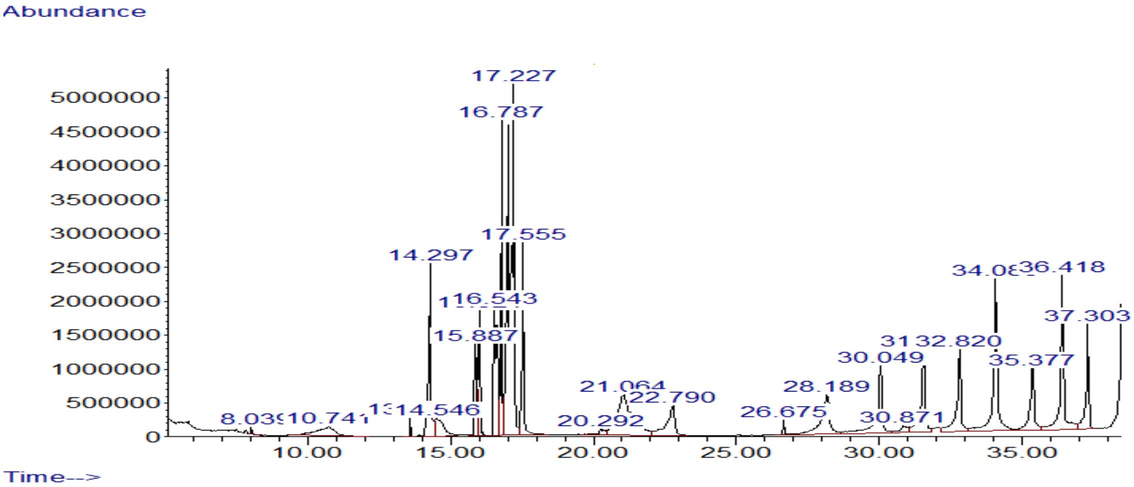

Figure 9: Gas Chromatography-Mass Spectrometer (GC-MS) of CSOB Biodiesel

Table 9: Fatty acid compositions of biodiesel.

S/N	**FFA Profile**		**Castor seed oil**
	Fatty Acid	Component	Composition (%)
1	Laureate	C_{12}	0.88
2	Myristeate	C_{14}	0.18
3	Palmiteate	$C_{16:0}$	10.23
4	Palmitileate	C16:2	1.14
5	Stearate	$C_{18:0}$	15.66
6	Oleate	$C_{18:1}$	61.4
7	Linoleate	$C_{18:2}$	10.51
	Total		100

3.8.3 FTIR Analysis of CSOB Biodiesel

Figure 10 shows the Fourier Transform Infra-red Spectrometer for the conversion of triglyceride of CSOB to methyl ester by catalyst. From the figure, the IR peak at 3008–3470.2cm^{-1} is attributed to the stretching of hydroxyl (OH) groups in the biodiesel. This functional group is predominant in biodiesel produced from natural seed oil biomass. This could be a result of better conversion of triglyceride. The IR peaks at 1380.5-1488.8cm^{-1} are assigned to the peaks of bending vibration of the O=C=O group. The two bands within the range of 2072.4–2922.2cm^{-1} and peak at 1740.7cm^{-1} on the IR spectra of reused catalyst are ascribed to the C-H stretching of the alkyl group and C=O stretching of the esters group, respectively. These bands occurred because of the unconverted triglyceride in the oils.

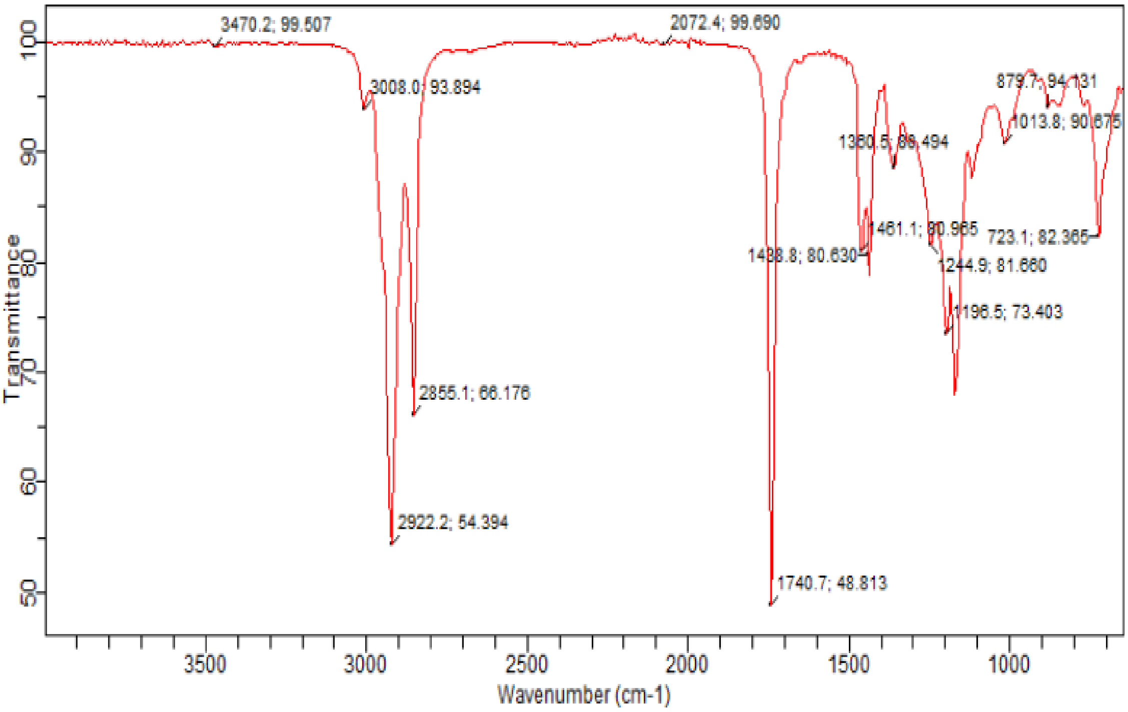

Figure 10: FTIR spectrum of biodiesel produced from castor seed oil.

4.0 Conclusion

The production of biodiesel from castor seed oil biomass using AASHA as a heterogeneous catalyst was investigated. The use of the AASHA catalyst enabled the oil to undergo direct transesterification without pretreatment, despite its high free fatty acid content. The effects of process parameters such as methanol/oil molar ratio, catalyst concentration, reaction temperature, time, and agitation speed on the biodiesel yield were studied. Optimization using response surface methodology (RSM) showed that the optimal conditions for maximum biodiesel yield (90.9%) were: methanol/oil molar ratio of 10.4:1, catalyst concentration of 2.19 wt%, reaction temperature of 63°C, reaction time of 1.5 hours, and agitation speed of 394 rpm. The properties of the produced biodiesel, such as density, viscosity, flash point, cetane number, and fatty acid composition, were found to be within the ASTM standards for biodiesel. The study demonstrates the potential of using AASHA as a cost-effective and environmentally friendly catalyst for the production of high-quality biodiesel from castor seed oil.

List of Abbreviations

AASHAA	*Afzelia Africana* seed husk ash
RSM	Response surface methodology
GC-MS	Gas Chromatography-mass spectrometry
FAME	Fatty acid methyl ester
ASTM	American Society for Testing and Materials
FTIR	Fourier Transform Infrared Spectroscopy
FFA	Free fatty acid
BET	Brunauer-Emmett-Teller
BJE	Barrett-Joyner-Halenda
SEM	Scanning electron microscopes

XRF	X-ray fluorescence
XRD	X-ray diffraction
CCD	Central Composite Design
CSOB	Castor Seed Oil Biodiesel

Declarations

Credit authorship contribution statement

E.E.M: Conceptualization. Wrote the original draft, Methodology. E.E.M and U.C.M: Validation, Resources, project administration, and review of manuscript.

Declaration of competing interest

The authors declare no conflict of interest.

Funding

The authors received no funding for this research.

Consent for publication

Not applicable

Ethics and Consent to Participate

Not applicable

Acknowledgement

The authors wish to thank the management and technical staff of the Departments of Chemical Engineering at Caritas University and Federal University Otuoke for administrative support.

References

Adebayo G.B., Ameen O.M. & Abass L.T. (2011). Physico-chemical properties of biodiesel produced from Jatropha Curcas oil and fossil diesel. Journal of Microbiology and Biotechnology Research, 1 (1), 12-16.

Ani I.J., Akpan U.G., Ezeh E.M., & Egbosiuba T C. (2024). Sorption – New Perspectives and Applications. - The Impact of Green Technology on Sorption Processes.

Atadashi, I.M., Aroua, M.K. & Aziz, A.A. (2010) High-quality biodiesel and its diesel engine application, a review. Renewable and Sustainable Energy Review, 14, 1999-2008.

Atadashi, I.M., Aroua, M. K., Abdul Aziz, R. & Sulaiman, N. M. N. (2012) The effects of catalysts in biodiesel production: A review. Renewable and Sustainable Energy Reviews, 16(5), 3456-3470.

Betiku, E., Okeleye, A. A., Ishola, N. B., Osunleke, A. S., Ojumu, T. V. (2019). Development of a Novel Mesoporous Biocatalyst Derived from Kola Nut Pod Husk for Conversion of Kariya Seed Oil to Methyl Esters: A Case of Synthesis, Modeling and Optimization Studies, Catal. Letters. 149, 1772–1787. doi:10.1007/s10562-019-02788-6. 2607.

Bohlouli, A., Mahdavian, L. (2019). Catalysts used in biodiesel production: a review Catalysts used in biodiesel production: a review. Biofuels, 1–14. doi:10.1080/17597269.2018.1558836.

Changmai, B., Laskar, I. B., Rokhum, L. (2019). Microwave-assisted synthesis of glycerol carbonate by the transesterification of glycerol with dimethyl carbonate using Musa acuminata peel ash catalyst, J. Taiwan Inst. Chem. Eng. 102, 276–282. doi: 10.1016/j.jtice.2019.06.014.

Chatterjee, S., Dhanurdhar, Rokhum, L. (2017). Extraction of a cardanol-based liquid bio-fuel from waste natural resource and decarboxylation using a silver-based catalyst, Renew. Sustain. Energy Rev. 72, 560–564. doi: 10.1016/j.rser.2017.01.035.

Cheng, J., Qiu, Y., Huang, R., Yang, W., Zhou, J., Cen, K. (2016). Biodiesel production from wet microalgae by using graphene oxide as a solid acid catalyst, Bioresour. Technol. 221, 344–349. doi: 10.1016/j.biortech.2016.09.064.

Dalvand, P., Mahdavian, L (2018). Calculation of the properties of biodiesel produced from castor seed byeg gshell catalyst. Biofuels. 9,705–710. doi:10.1080/17597269.2017.1302668.

Da Silva César, A., Conejero, M. A., Barros Ribeiro, E. C., Batalha, M. O. (2019). Competitiveness analysis of “social soybeans” in biodiesel production in Brazil, Renew. Energy. (2019) 1147–1157. doi: 10.1016/j.renene.2018.08.108.

De Oliveira, F. C., Coelho, S. T. (2017). History, evolution, and environmental impact of biodiesel in Brazil: A review, Renew. Sustain. Energy Rev. 75, 168–179.doi: 10.1016/j.rser.2016.10.060.

Delzeit, R. (2019). Using Used Cooking Oil (UCO) for biofuel production: Effects on global land use and interlinkages with food and feed production., (2019).

Esonye, C., Onukwuli, O. D., Ofoefule, A. U. (2019). Optimization of production from prunus amygdalus seed oil using response surface methodology and artificial neural networks, Renewable Energy 130 (2019) 62–71, https://doi.org/10.1016/j.renene.2018.06.036.

Eze, C. N., Onukwuli, O. D., Ude, C. N., Gbasouzor, A. I. (2022). Biodiesel synthesis from waste canarium schweinfurtii oil (WCSO) catalyzed by thermal reinforced clay and its kinetics evaluation. Cleaner Materials, 6. https://doi.org/10.1016/j.clema.2022.100145.

Ezeh, E. M., Agu, P C.,& Aworabhi E (2024). Biological Treatment Techniques for Sewage: Aerobic and Anaerobic Processes: IntechOpen (Sewage- Management and Treatment Techniques). DOI: http//dx.doi.org/10.5772/intechopen.1006097.

Ezekoye V. Adinde R., Ezkoye D. and Ofomatah A. (2019) Syntheses and characterization of biodiesel from citrus sinensis seed oil. Scientific African, 6, https://doi.org/10.1016/j.sciaf.2019.e00217.

Flach, B., Lieberz, S., Rondon, M., Williams, B., Teiken, C. (2015). GAIN Report: EU-28 Biofuels Annual 2015, (2015) 14–21. http://gain.fas.usda.gov/Recent GAIN 2216 Publications/Biofuels Annual_The Hague_EU-28_7-15-2015.pdf.

Georgogianni, K. G., Katsoulidis, A. P., Pomonis, P. J. & Kontominas, M. G. (2009) Transesterification of soybean frying oil to biodiesel using heterogeneous catalysts: Fuel Processing Technology, 90, 671-676.

Gusniah, A., Veny, H., Hamzah, F. (2019). Ultrasonic Assisted Enzymatic Transesterification for Biodiesel Production, Ind. Eng. Chem. Res. 58, 581–589. doi: 10.1021/acs.iecr.8b03570.

International Renewable Energy Agency (IRENA), Global Energy Transformation: A Roadmap to 2050, (2018). doi:Doi 10.1002/(Sici)1097-0029(19990915)46:6<398::Aid- Jemt8>3.0.Co;2-H.

Jambulingam, R., Shalma, M., Shankar, V. (2019). Biodiesel production using lipase immobilised functionalized magnetic nano catalyst from oleaginous fungal lipid, J. Clean. Prod. 215 (2019) 245–258. doi: 10.1016/j.jclepro.2018.12.146.

Jayaraman, J., Alagu, K., Appavu, P., Joy, N., Jayaram, P., Mariadoss, A. (2020). Enzymatic production of biodiesel using lipase catalyst and testing of an unmodified compression ignition engine using its blends with diesel. Renew. Energy. 145, 399–407. doi:10.1016/j.renene.2019.06.061.

Kim, K. H., Lee, O. K., Lee, E. Y. (2018). Nano-immobilized biocatalysts for biodiesel production from renewable and sustainable resources. Catalysts. 8 (2018). doi:10.3390/catal8020068.

Lathiya, D. R., Bhatt, D. V., Maheria, K. C. (2018). Synthesis of sulfonated carbon catalyst from waste orange peel for cost-effective biodiesel production, Bioresour. Technol. Reports. 2, 69–76. doi:10.1016/j.biteb.2018.04.007.

Ma, Y., Wang, Q., Sun, X., Wu, C., Gao, Z. (2017). Kinetics studies of biodiesel production from waste cooking oil using $FeCl_3$-modified resin as a heterogeneous catalyst. Renew. Energy. 107, 522–530. doi: 10.1016/j.renene.2017.02.007.

Malani, R. S., Umriwad, S. B., Kumar, K., Goyal, A., Moholkar, V. S. (2019). Ultrasound-assisted enzymatic biodiesel production using a blended feedstock of non–edible oils: Kinetic analysis. Energy Convers. Manag. 188, 142–150. doi:10.1016/j.enconman.2019.03.052.

Moazeni, F., Chen, Y. C., Zhang, G. (2019). Enzymatic transesterification for biodiesel production from used cooking oil, a review, J. Clean. Prod. 216, 117–128. doi:10.1016/j.jclepro.2019.01.181.

Moser, B. R. (2009). Biodiesel production, properties and feedstocks. In Vitro Cell Development Biology-Plant, 45, 229-266.

Onukwuli, O. D. And Ude C. N. (2018). Kinetics of African pear seed oil (APO) methanolysis catalyzed by phosphoric acid-activated kaolin clay. Applied Petrochemical Research, https://doi.org/10.1007/s13203-018-0210-0

Orwa, C., Mutua, A., Kindt, R., Jamnadass R., Anthony. S. (2009). Agroforestry Database: a tree reference and selection guide version 4.0(http://www.worldagroforestry.org/sites/treedbs/treedatabases.asp)

Pathak, G., Das, D., Rajkumari, K., Rokhum, L. (2018). Exploiting waste: Towards a sustainable production of biodiesel using: Musa acuminata peel ash as a heterogeneous catalyst, Green Chem. 20, 2365–2373. doi:10.1039/c8gc00071a.

Sebastian, J., Muraleedharan, C., Santhiagu, A. (2017). Enzyme-catalyzed biodiesel production from rubber seed oil containing high free fatty acid. Int. J. Green Energy. 14, 687–693. doi:10.1080/15435075.2017.1318754.

Septiani U., RezaAudina P. and Novesar J. (2016) Synthesis of zeolite ZSM-5 from rice husk ash as catalysts in vegetable oil transesterification for biodiesel production. Der Pharmacia Lettre, 8 (19), 86 - 91Taher, H., Nashef, E., Anvar, N., Al-Zuhair, S. (2019). Enzymatic production of biodiesel from waste oil in ionic liquid medium. Biofuels, 10, 463–472. doi:10.1080/17597269.2017.1316145.

Talha, N. S., Sulaiman, S. (2016). Overview of catalysts in biodiesel production, ARPN J. Eng. Appl. Sci. 11, 439–442.

Ude, C. N., Onukwuli, O. D. (2019a). Kinetic modelling of transesterification of gmelina seed oil catalyzed by alkaline activated clay (NaOH/clay) catalyst. Reaction Kinetics, Mechanisms and Catalysis (2019) 127:1039–1058. https://doi.org/10.1007/s11144- 019-01604-x

Ude C. N. and Onukwuli O. D. (2019b) African pear seed oil methanolysis catalyzed by thermally activated clay. Journal of Engineering and Applied Sciences, 15(1), 88 – 98.

Ude, C. N., Onukwuli, O. D., Umeuzuegbu, J. C., Chukwuka, C. C. (2020). Heterogeneously catalyzed methanolysis of gmelina seed oil to biodiesel. Chemical Engineering and Technology, 44(1). DOI: 10.1002/ceat.202000080.

Ume C. S, Esonye C, Ikechukwu N. B, Ani A.K, Onyekwere I.J, Chukwu E.G, Ude C.N, Ezeannagha C.B, Ezeh E.M, and Uwaoma O.A(2024). Bioresource integration approach of sustainable green-diesel production from waste mutton using waste goat bone as bio heterogeneous catalyst Thermal Science and Engineering Progress, https://doi.org/10.1016/j.tsep.2024.102711.

Wancura, J. H. C., Rosset, D. V., Tres, M. V., Oliveira, J. V., Mazutti, M. A., Jahn, S. L. (2018). Production of biodiesel catalyzed by lipase from Thermomyces lanuginosus in its soluble form. Can. J. Chem. Eng. 96. doi:10.1002/cjce.23146.

List of Figure

List of Tables